Alignment for Comprehensive Two-Dimensional Gas Chromatography with Dual Secondary Columns and Detectors

(Article begins on next page)

15 October 2023

UNIVERSITÀ DEGLI STUDI DI TORINO

Alignment for Comprehensive Two-Dimensional Gas Chromatography with Dual Secondary Columns and Detectors (GCx2GC)

Stephen E. Reichenbach,[*] Davis W. Rempe,[*] Qingping Tao,[†] Davide Bressanello,[‡] Erica Liberto,[‡] Carlo Bicchi,[‡] Stefano Balducci,[§] Chiara Cordero[‡]

*University of Nebraska – Lincoln, Lincoln NE 68588-0115, USA

†GC Image, LLC, Lincoln NE 68505-7403, USA

‡Università degli Studi di Torino, I-10125 Torino, Italy

§La Sapienza University, Rome, Italy

ABSTRACT: In each sample run, comprehensive two-dimensional gas chromatography with dual secondary columns and detectors (GCx2GC) provides complementary information in two chromatograms generated by its two detectors. For example, a flame ionization detector (FID) produces data that is especially effective for quantification and a mass spectrometer (MS) produces data that is especially useful for chemical-structure elucidation and compound identification. The greater information capacity of two detectors is most useful for difficult analyses, such as metabolomics, but using the joint information offered by the two complex two-dimensional chromatograms requires data fusion. In the case that the second columns are equivalent but flow conditions vary (e.g., related to the operative pressure of their different detectors), data fusion can be accomplished by aligning the chromatographic data and/or chromatographic features such as peaks and retention-time windows. Chromatographic alignment requires a mapping from the retention times of one chromatogram to the retention times of the other chromatogram. This paper considers general issues and experimental performance for global two-dimensional mapping functions to align pairs of GCx2GC chromatograms. Experimental results for GCx2GC with FID and MS for metabolomic analyses of human urine samples suggest that low-degree polynomial mapping functions out-perform affine transformation (as measured by root-mean-square residuals for matched peaks) and achieve performance near a lower-bound benchmark of inherent variability. Third-degree polynomials slightly out-performed second-degree polynomials in these results, but second-degree polynomials performed nearly as well and may be preferred for parametric and computational simplicity as well as robustness.

This work demonstrates global transformation functions to align the retention times of chromatograms acquired by comprehensive two-dimensional gas chromatography with one primary column and two parallel secondary columns (GCx2GC), with a flame ionization detector (FID) for one secondary column and a mass spectrometer (MS) for the other, i.e., GCx2GC-FID/MS. GCx2GC increases separation efficiency and information capacity (*1,2,3,4*), but the two resulting chromatograms may exhibit different retention-time patterns. Then, a retention-times transformation function is required to map between the data-points and/or features such as peaks in the two chromatograms.

Seeley et al. proposed a GCx2GC system with two secondary columns with different selectivity characteristics, each connected with a separate FID, to "increase the resolution and qualitative information supplied by comprehensive two-dimensional gas chromatographic analysis." (*1*)p.

450 They demonstrated results for mixtures of volatile organic compounds (VOCs) and complex gaseous samples, including exhaled breath (*2*). Peroni et al. (*5,6*) used multiple identical second columns to achieve optimum carrier gas velocity, but employed only a single FID. Nicolotti, Bressanello, and Cordero similarly used identical second columns for improved gas linear velocities in both chromatographic dimensions, but connected one column to a FID and the other column to a MS with auxiliary flow/pressure controller. (*3*) In a study of metabolic profiling and fingerprinting with mice urine samples, they concluded that "working in close-to-optimal 2D linear velocities and a doubled secondary column loading capacity, showed positive effects on overall system orthogonality, resolution, and fingerprinting accuracy." (*4*)p. 276 The benefits of using both FID and MS in a single run include complementary data, with improved quantification compared to MS alone

and improved compound identification compared to FID alone, and the ability to cross-validate results.

GCx2GC-FID/MS systems produce two complementary chromatograms for each sample run. The greater information capacity of two detectors is especially useful for difficult analyses, such as metabolomics, but using the joint information offered by the two chromatograms requires data fusion. In the case that the second columns are equivalent but flow conditions vary (e.g., related to the detectors' different operative pressures), data fusion can be accomplished by aligning the chromatographic data and/or chromatographic features such as peaks and retention-time windows. In a GCx2GC-FID/MS system without auxiliary flow/pressure control at the outlet of the secondary column for the MS, there are differences between the two-dimensional (2D) retention-times patterns of the two detectors. (*3*) Outlet pressure control adds carrier volumetric flow to reduce these differences, but alignment still is required. The coherence of 2D patterns produced by FID/MS parallel detection was handled by affine transformation implemented in template matching (*4*) for analysis of mice urine metabolome, but with manual intervention to cross-align FID and MS template patterns. More effective alignment could reduce or eliminate the need for manual intervention.

A fundamental distinction amongst alignment methods is whether the underlying model is global or local, i.e., whether the geometric differences between chromatograms are characterized by a single function for the entire chromatogram or by a combination of many functions for different regions of the chromatogram. A brief review of local methods used to align GCxGC data is included in the Supporting Information (7-15). Global functions may be able to capture systemic properties and structure that underlie retention-time differences. On the other hand, local functions may be able to capture retention-time variations that are not related to systemic properties and structure. Local functions typically offer greater representational power than simple global functions, which allows them to capture small-scale variations, but also are more susceptible to overfitting of confounding input differences (e.g., compositional differences, artifacts, and noise) and so may be less robust than global functions. Global functions with many parameters have unlimited representational power but also have greater susceptibility to overfitting. Finally, global functions with few parameters are computationally simple. For these reasons, the ideal solution is an alignment method based on a simple global model with few parameters that is able to effectively capture chromatographic differences. Of course, if the chromatographic differences are too complex, a simple global function with few parameters may prove ineffective for modeling those differences. In such circumstances, local functions may be required.

In an early study of global functions for modeling chromatographic differences in GCxGC data, Ni et al. (*16*) found that four-parameter separable shift-and-scale and six-parameter bivariate affine (shift, scale, and shear) functions were effective for modeling retention-time differences related to oven temperature ramp rate and inlet gas pressure. They noted that these functions, optimized for least-squares fit, would be effective for pattern matching

and normalizing retention times to retention indices. Van Mispelaar (*17*) parameterized a global bivariate second-degree polynomial function (with 12 parameters) using the locations of six peaks (supplying the minimum number of constraints for the second-degree polynomial), then used bilinear interpolation to resample the data values.

The goal of this research is to evaluate the performance of simple global alignment models for GCx2GC in order to determine their representational effectiveness. As described in the Experimental Section, performance is quantified by the root-mean-square error (RMSE) for retention times of matched peaks in paired FID and MS chromatograms from a single GCx2GC run. The performance benchmark is the RMSE between matched peaks for the same detector (i.e., FID with FID and MS with MS) in consecutive replicate runs, with the expectation that consecutive replicate runs exhibit negligible sample and chromatographic differences. Then, small misalignments for consecutive replicate runs can be deemed noise, thereby providing a performance benchmark. If the performance of a simple global method to align FID and MS chromatograms from GCx2GC can approach the benchmark, then the residual differences can be attributed to noise rather than chromatographic misalignment. The experiments employed cross-validation to evaluate three simple global 2D alignment methods: affine, second-degree polynomial, and third-degree polynomial transformations.

■ EXPERIMENTAL SECTION

Samples. The urine samples were gathered for the Italian Diabetes Exercise Study 2 (IDES_2), which is assessing the effect of a behavioral intervention strategy on the promotion and maintenance of physical activity in adults with type 2 diabetes. IDES_2 is a randomized clinical trial that monitors objective measurable changes in sedentary time and physical activity over a 3-year period after behavioral intervention as compared with usual care. The study also monitors physical fitness, modifiable cardiovascular risk factors (HbA1c, lipids, blood pressure, C-reactive protein), and health related quality of life. The samples analyzed by GCx2GC are for the first and fourth quartile of physical activity objectively measured at baseline. Sample preparation followed a standard derivatization protocol of oximation/silylation. (*18*) Derivatization reagents: O-methylhydroxylamine hydrochloride (MOX) and N-methyl-N-(trimethylsilyl)trifluoroacetamide (MSTFA), and HPLC-grade solvents: methanol, pyridine, n-hexane, and dichloromethane, were supplied by Sigma-Aldrich (Milan, Italy).

Calibration standards of pyruvic acid, lactic acid, malonic acid, succinic acid, malic acid, 2-ketoglutaric acid, hippuric acid, L-alanine, L-valine, glycine, L-threonine, L-tyrosine, creatinine, phenylalanine, xylitol, ribitol, glycerol, fructose, galactose, glucose, mannitol, and myo-inositol; and the internal standard (ISTD) 4-fluorophenylalanine were from Sigma-Aldrich (Milan, Italy). Calibration solutions for quantitative determination of relevant analytes were prepared as in a previous protocol (*4*) at 2 mg/L, 10 mg/L, 50 mg/L, and 100 mg/L. The ISTD for data normalization and quality control, 4-Fluorophenylalanine, was at 10 mg/L.

Instrumentation. Separations were performed with an Agilent 6890-5975C GC-MS fast quadrupole. The first-dimension (^{1}D) column was SE52 (30m x 0.25 mm internal diameter (ID) x 0.25 μm film thickness (df)) and the two parallel second-dimension (^{2}D) columns were OV1701 (1.4 m x 0.10 mm ID x 0.10 μm df). Columns were from Mega (Legnano, Milan, Italy). The carrier gas was helium with initial head pressure 296 kPa (constant flow). The modulation period was 5 sec with pulse time 0.350 msec. The FID acquisition frequency was 100 Hz and the MS performed full scans (50–350 m/z) at 24 Hz. The oven programming was 50°C (1 min) to 300°C (10 min) at 4.0°C/min. A microfluidic 3-port splitter (Sil-flow™- SGE Ringwood, Victoria, Australia) split the flow from the ^{1}D column into the two parallel ^{2}D columns where the first 0.60 m were wrapped together in the loop-type thermal modulator (Zoex Corporation, Houston, TX). A deactivated, restrictor capillary (0.17 m x 0.1 mm ID) was connected to the outlet of the ^{2}D column for the MS.

Data Preprocessing. Preprocessing was performed with GC Image GCxGC Edition Software (R2.6 pre-release, GC Image, LLC, Lincoln NE, USA). The preprocessing operations were start-time adjustment, modulation-phase rotation, baseline correction, and peak detection ([19]). For any two chromatograms, corresponding peaks were paired by preliminary bi-directional template matching and then interactive selection using a new graphical user interface (GUI) for interactive template matching and transformation. ([20]) For the calibration samples, 25 peaks were paired. For the urine samples, 156 peaks were paired. For each set of N_p paired peaks, the retention times of the peaks in the target chromatogram are denoted (x_i, y_i) and the peaks in the reference chromatogram are denoted (x'_i, y'_i) where i is the peak index from 1 to N_p.

Evaluation Metric. The difference of retention times for paired peaks in two chromatograms is two dimensional, with a difference in each chromatographic dimension. The RMSE is computed as the square roots of the means of the squared relative retention-times differences:

$$RMSE = \left(\sqrt{\frac{1}{N_p}\sum_1^{N_p}(x_i - x'_i)^2}, \sqrt{\frac{1}{N_p}\sum_1^{N_p}(y_i - y'_i)^2} \right). \quad (1)$$

The retention-time differences in each dimension also are expressed relative to the average detected peak-width in that dimension (w_x, w_y), based on the logic that the peak widths are fundamental to chromatographic resolution. The relative RMSE is:

$$RRMSE = \left(\frac{RMSE_x}{w_x}, \frac{RMSE_y}{w_y} \right). \quad (2)$$

Transformation Models. Experiments evaluated initial misalignment (i.e., no transformation) and the performance of three transformation models, each generalizing the previous model with additional parameters. For each model, if the number of peak-pairs over-constrains the model, the model parameters are determined to minimize the RMSE for the peak-pairs set ([21]).

For notational completeness, the identity transformation, which gives the initial misalignment, is defined as:

$$f_0(x, y) = (x, y). \quad (3)$$

The affine transformation is linear scaling and shearing plus translation:

$$f_1(x, y) = \left(t_x + s_x x + h_x y, \; t_y + h_y x + s_y y \right) \quad (4)$$

where (s_x, s_y) are the scale parameters, (h_x, h_y) are the shear parameters, and (t_x, t_y) are the translation parameters. The affine transform preserves parallel lines and distance ratios. A minimum of three non-collinear two-dimensional peak-pairs (one peak of each pair from each chromatogram) are required to parameterize the affine transformation.

The second-degree polynomial adds three additional terms in each dimension:

$$f_2(x, y) = (t_x + s_x x + h_x y + a_x xy + b_x x^2 + c_x y^2, t_y + h_y x + s_y y + a_y xy + b_y x^2 + c_y y^2). \quad (5)$$

A minimum of six peak-pairs are required to parameterize the second-degree polynomial transformation.

The third-degree polynomial adds four additional terms in each dimension:

$$f_3(x, y) = (t_x + s_x x + h_x y + a_x xy + b_x x^2 + c_x y^2 + \alpha_x x^2 y + \beta_x xy^2 + \gamma_x x^3 + \delta_x y^3, t_y + h_y x + s_y y + a_y xy + b_y x^2 + c_y y^2 + \alpha_y x^2 y + \beta_y xy^2 + \gamma_y x^3 + \delta_y y^3). \quad (6)$$

A minimum of ten peak-pairs are required to parameterize the third-degree polynomial transformation.

For GCx2GC data, these models could be simplified by presuming that the first-column retention-times are identical and so transforming only the second-column retention times. However, for completeness, the experimental results shown here use the general two-dimensional models.

Because each successive transformation model subsumes the representational power of the lower-order models, performance is monotonically non-decreasing with order; i.e., higher-order polynomials always do at least as well as lower-order polynomials for a given set of peak-pairs. With no limit on the polynomial degree, arbitrarily large peak-pairs sets can be transformed with no residual error. However, if a lower-order polynomial successfully models the actual chromatographic transformation, then additional parameters merely increase overfitting and incur additional computation. So, for robustness and computational efficiency, lower-degree polynomials are preferred if they are representationally effective

Evaluation Methodology. Given two chromatograms, a set of corresponding peak-pairs is used to determine the optimal transformation, so the RMSE of those points after the transformation is a biased indicator of performance for other points. In particular, the transformation is the best fit for the specific peak-pairs, including noise inherent in their peak locations. That the transformation fits the noise as well as the relevant chromatographic differences is called overfitting. Constraining the transform with many points tends to attenuate overfitting, but it is important to assess the level of overfitting, particularly for small peak-pairs sets.

Cross-validation can be used to provide an unbiased estimate of the transformation performance. In cross-validation, a peak-pairs set is partitioned into a training set, which is used to determine the transform, and a testing set, which is used to independently evaluate performance. To account for variability, results over multiple rounds of cross-validation, each performed using randomly generated partitions of the peak-pairs set, are averaged. Gros et al.
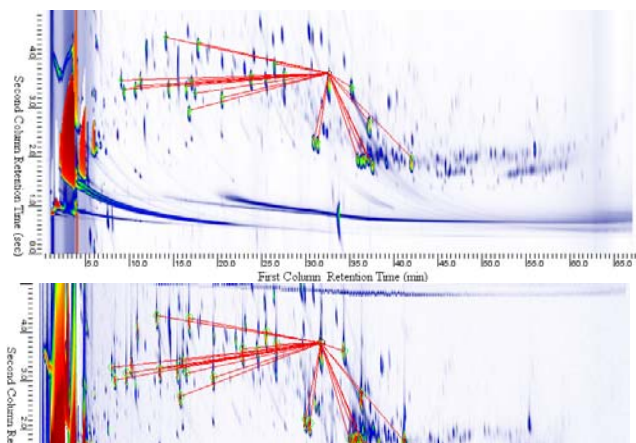
(*13*) used leave-one-out cross-validation (i.e., training sets with all but one peak-pair), but the size of the training set can be varied to assess performance relative to the number of peak-pairs used to determine the transformation. Performance measures for both the training and testing sets are reported.

Each cross-validation result is computed across random partitions, for each transformation method (including no transformation), for both the training set and the testing set, at each training set size from 3 peak-pairs (the minimum size for the affine transformation) to the total number of peak-pairs (which does not allow for a testing set), for both directions of transformation (i.e., switching the target and reference chromatograms). The RMSE for each cross-validation result is computed as:

$$\overline{RMSE} = \left(\sqrt{\frac{1}{KN_p}\sum_1^K\sum_1^{N_p}(x_i - x_i')^2}, \sqrt{\frac{1}{KN_p}\sum_1^K\sum_1^{N_p}(y_i - y_i')^2} \right)$$
(7)

where K is the number of iterations of random partitioning. For the graphs shown in Results and Discussion, K=100 and the $\overline{RMSE}$ values for the transformations in both directions of the same cross-validation partition are averaged. Additional statistics related to worst-case performance (maximum RMSE) are included in the Supporting Information.

Performance Benchmarks. The goal is a transformation between FID and MS chromatograms from the same GCx2GC run. The performance of each transformation model for this task is compared to a benchmark computed as the RMSE between matched peaks for the same detector (i.e., FID with FID and MS with MS) in consecutive replicate runs. Consecutive replicate runs have negligible sample and chromatographic differences (regarded as noise), so any transformation model for them should provide only negligible reductions in RMSE. If the performance of a transformation model to align FID and MS chromatogram pairs can approach the benchmark of consecutive replicate runs, then the residual differences can be attributed to noise rather than chromatographic misalignment.

Aligning Chromatographic Features and Data. Transformation models are sufficient to map retention-times of peaks, windows, or other features from one chromatogram to align with another chromatogram. However, mapping data values in one chromatogram (or an entire chromatogram) to align with another chromatogram requires additional steps of resampling (and interpolation or approximation). The additional steps to align data values are not discussed here, but the alignment RMSE of data points left out during cross-validation is an indicator of retention-time mapping quality for data points which are not in the training set.

The computation required for low-degree polynomial mapping is small. For example, on a computer with an Intel i7-4770 CPU with 4 cores at 3.4GHz and 16GB RAM and Microsoft Windows 10 64-bit OS, Java bytecode execution required about 0.018 msec for optimal fitting of a second-degree polynomial to 156 matched peak-pairs (which is a fairly large number of alignment peaks) and about 0.067 msec to apply the second-degree polynomial to remap the retention times of 156 peaks. Presumably, compiled code would be faster.

■ RESULTS AND DISCUSSION

Results for Calibration Chromatograms. The first experiments presented here evaluated calibration runs with a set of informative target metabolites to be quantified in the human urine samples. Figure 1 shows images of the FID and MS chromatograms from one of the calibration runs (with concentration 100 mg/L). Open green circles indicate the analyte peaks used for alignment experiments. Red lines connect each analyte peak to the ISTD peak, which is indicated with a black circle. Peak identities and retention times are provided as Supporting Information.

The average peak widths, computed as the second-central moments (i.e., standard deviations), were determined from these peaks in six FID and MS chromatograms of three consecutive replicate calibration runs. The average peak standard-deviation widths were about $^1\sigma$=0.060 min and $^2\sigma$= 0.085 sec. In ^{1}D, the standard-deviation peak width was slightly less than the modulation cycle, P_M=0.083 min, which has implications for the alignment benchmark. The standard deviation for randomly distributed positions over a single modulation interval is $12^{-\frac{1}{2}}\times P_M$, which is about 0.024 min (or $0.4\times^1\sigma$) for these data. This is the RMS noise level from the sampling effect of modulation. In ^{2}D, the average peak width is about 8.5 times the sampling rate for the FID data and twice the sampling rate for the MS data. The RMS noise level from
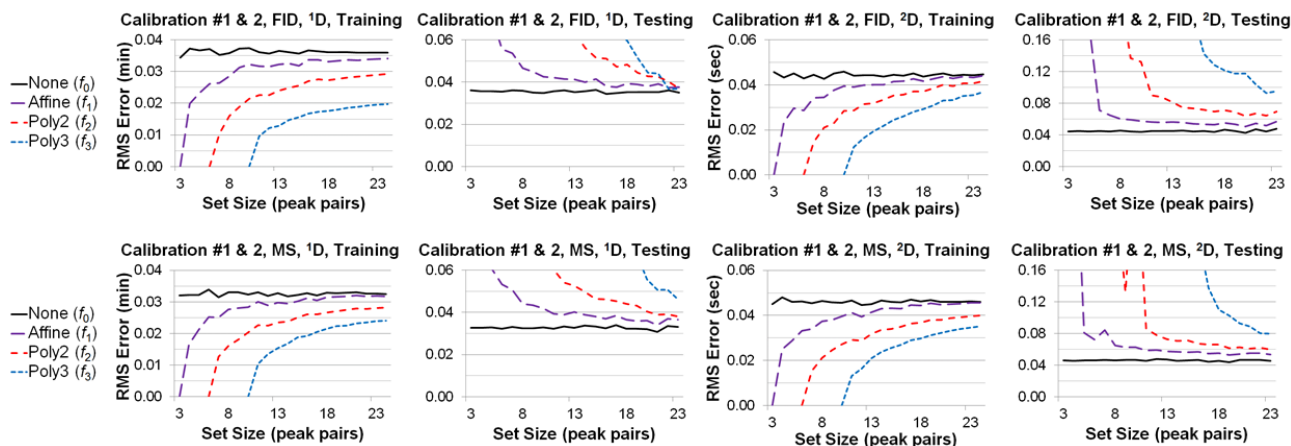
Figure 2: Cross-validation RMSE results as a function of the training set size for alignment of consecutive, replicate calibration chromatograms from the same detector. Columns from left to right are for ^1D with the training set, for ^1D with the testing set, for ^2D with the training set, and for ^2D with the testing set. The top row is for the FID chromatograms of calibration runs #1 and #2 and the bottom row is for the MS chromatograms of calibration runs #1 and #2.

detector sampling is about 0.003 sec (or $0.03 \times ^2\sigma$) for the FID data and 0.012 sec (or $0.14 \times ^2\sigma$) for the MS data.

The benchmarks for the calibration runs were evaluated for consecutive replicate runs with respect to the same detector. As can be seen in Figure 2, for consecutive replicate runs, there was a small misalignment of peak-pairs (shown by the solid black lines labeled "None (f_0)"): for ^1D, about 0.035 min or $0.6 \times ^1\sigma$; and, for ^2D, about 0.045 sec or $0.5 \times ^2\sigma$. In ^1D, the misalignment is only a little more than the stochastic modulation-sampling noise level (0.024 min). With the results in the Supporting Information, the ^2D misalignment averaged slightly more for MS than FID (0.045 sec versus 0.039 sec), which is in line with the difference in detector sampling noise (a difference of 0.009 sec). When aligning FID and MS chromatograms from the same run, we would like to approach these benchmarks: 0.035 min in ^1D and 0.045 sec in ^2D.

The expectation that the misalignment in chromatograms from the same detector for consecutive replicate runs is due to noise is supported by the observation that the global transformations produced no improvements in alignment of the testing-set peaks. Figure 2 illustrates the performance of the alignment methods for both the training and testing sets (shown as colored, dashed lines). When the models are not over-constrained (peak-pairs sets of size 3, 6, and 10, respectively, for f_1, f_2, and f_3), they are able to perfectly align the peak-pairs in the training set. Those models are computed to fit the retention-times noise in the training-set peaks as well as any underlying transformation, so this perfect performance is misleading, as evidenced by the performance for the testing-set peaks. As more peak-pairs are included in the training set (which reduces overfitting to noise), the performance for the training set worsens, but the more meaningful performance for the testing-set peaks improves. However, the performance gains from using additional peak-pairs to optimize the model diminish as the model is more and more constrained; and, even with all but one of the peaks in the training set, none of the models improves alignment for the testing set for consecutive replicate runs.
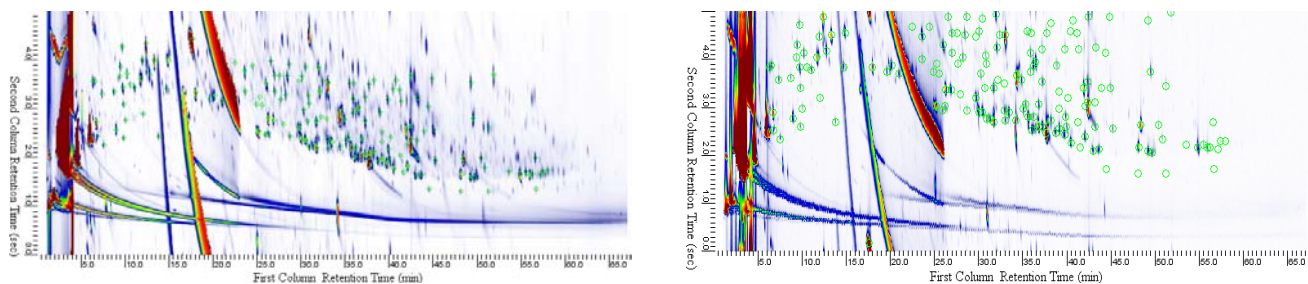
Figure 4: Two chromatograms from GCx2GC analysis of a urine sample, (A) FID on the left and (B) MS on the right. Peaks in the 156 peak-pairs set are indicated with open circles.

Figure 3 illustrates the performance for aligning the two chromatograms from a GCx2GC-FID/MS calibration run. As can be seen in the second of the four graphs, for ^{1}D, none of the models yields any improvement in the testing set, but this is expected because both the FID and MS chromatograms were generated for the same ^{1}D separation. Note also that the ^{1}D misalignment is approximately equal to the stochastic modulation sampling noise level

depth analyses are presented next in the results for urine samples, for which a larger peak-pairs set with wider retention-times ranges is used.

Results for Urine Sample Chromatograms. Figure 4 shows images of the FID and MS chromatograms from a GCx2GC analysis of a urine sample. Open green circles indicate the analyte peaks used for the alignment experiments. This peak-pairs set is more than six times larg-
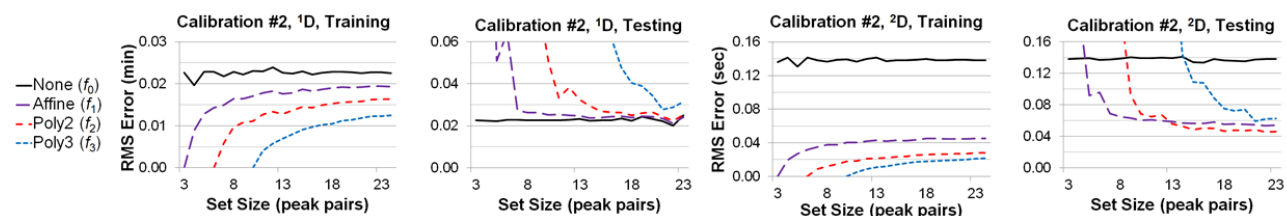

Figure 3: Cross-validation RMSE results as a function of the training set size for alignment of GCx2GC calibration chromatograms (from different detectors). Columns from left to right are for ^{1}D with the training set, for ^{1}D with the testing set, for ^{2}D with the training set, and for ^{2}D with the testing set. The rightmost graph demonstrates the effectiveness of the transformations.

(0.024 min). For ^{2}D, as seen in the right-most graph, all of the transformation models significantly improved alignment from about 0.14 sec (or $1.6 \times ^2\sigma$) before transformation to about 0.06 sec (or $0.7 \times ^2\sigma$) or less, with the second-degree polynomial approaching the benchmark of 0.045 sec. The performance of the third-degree polynomial is slightly worse than the benchmark; however, the peak-pairs set for the calibration data may not be large enough to provide robust constraints and is somewhat limited in covering the retention-times space, so more in-

er than the calibration peak-pairs set, with a wider retention-times distribution.

Figure 5 shows the alignment results for consecutive replicate runs of one of the urine samples, which are used to establish benchmarks. For ^{1}D, the benchmark is about 0.03 min (or about $0.5 \times ^1\sigma$); and, for ^{2}D, the benchmark is about 0.03 sec (or about $0.35 \times ^2\sigma$) for the MS (which has a lower sampling frequency than the FID). These values are slightly less than the benchmarks for the calibration peaks (but still above the level of stochastic noise from sam-
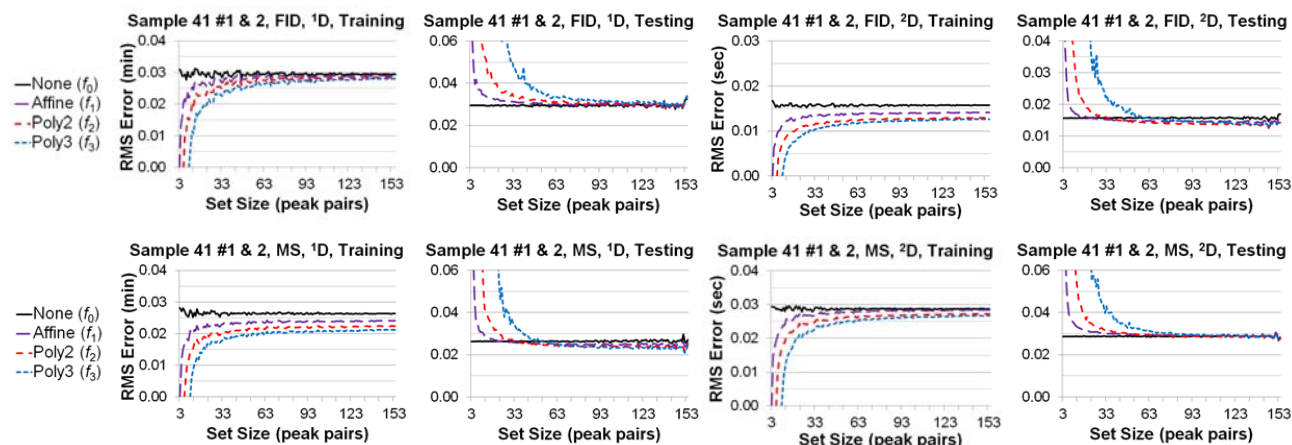

Figure 5: Cross-validation RMSE results as a function of the training set size for alignment of consecutive, replicate urine sample chromatograms from the same detector. Columns from left to right are for ^{1}D with the training set, for ^{1}D with the testing set, for ^{2}D with the training set, and for ^{2}D with the testing set. The top row is for the FID chromatograms of sample 41, runs #1 and #2, and the bottom row is for the MS chromatograms of sample 41, runs #1 and #2.
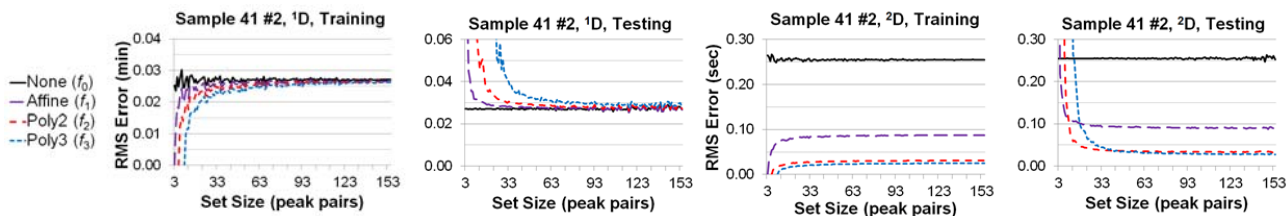
Figure 6: Cross-validation RMSE results as a function of the training set size for alignment of GCx2GC urine sample chromatograms (from different detectors). Columns from left to right are for ^{1}D with the training set, for ^{1}D with the testing set, for ^{2}D with the training set, and for ^{2}D with the testing set. The rightmost graph demonstrates the effectiveness of the transformations.
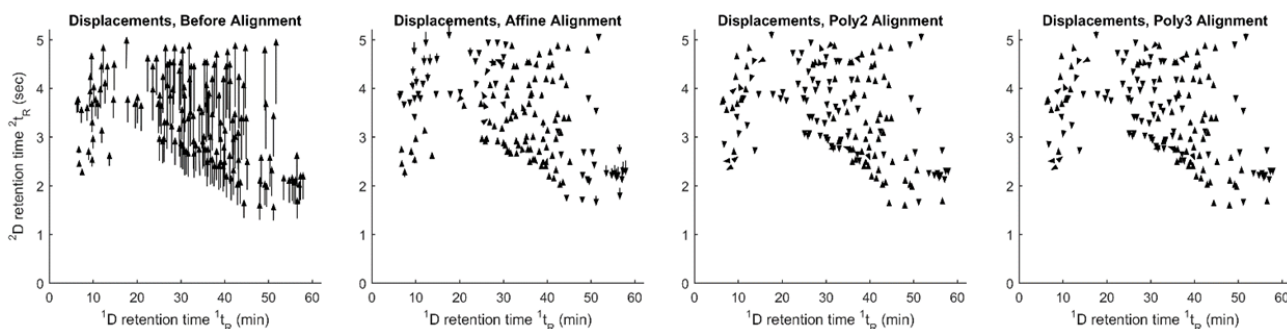

Figure 7: Misalignment vectors (from FID to MS) for 156 peak pairs in chromatograms from GCx2GC analysis of a urine sample. Columns from left to right are

pling), a difference that seems related to the larger, more intense peaks in the calibration sample. As seen in the results for the calibration
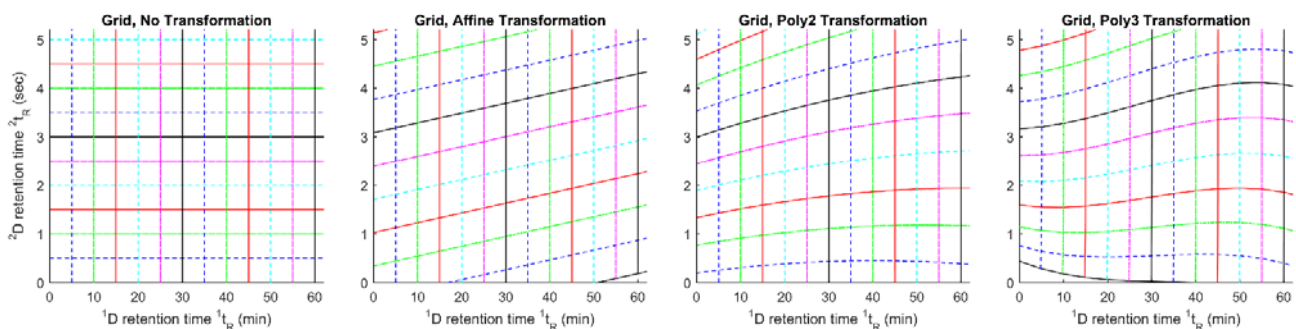

Figure 8: Transformation of grid lines using the models derived for Figure 7 (FID to MS mapping for GCx2GC analysis of a urine sample). Columns from left to right are for the four alignment transformations: none (f_0), affine (f_1), second-degree polynomial (f_2), and third-degree polynomial (f_3).

samples, none of the transformation models produced any improvement in alignment of consecutive replicate runs.

Figure 6 shows the alignment performance for the two chromatograms from a GCx2GC-FID/MS run of a urine sample. For ^{1}D, the misalignment of the FID and MS chromatograms is at the benchmark (about 0.03 min or $0.5 \times {}^1\sigma$) without transformation and, as expected, none of the models reduces misalignment. For ^{2}D, the misalignment before transformation is large, about 0.25 sec or $2.9 \times {}^2\sigma$, about eight times the benchmark. All of the transformation models significantly improve alignment.

As seen in the right-most graph in Figure 6, affine transformation reduces misalignment by about two-thirds, to 0.08 sec (or $0.9 \times {}^2\sigma$), but does not achieve the benchmark. Both polynomial transformations reduce misalignment to about 0.03 sec (or $0.35 \times {}^2\sigma$), which is the benchmark for consecutive replicate sample runs. The second-degree polynomial does not approach its peak performance until there are nearly 30 points in the training set, although it outperforms affine transformation with as few as 9 or 10 points. The third-degree polynomial requires nearly 20 points in the training set to outperform affine transformation and requires nearly 50 points to outperform the second-degree polynomial. Even when the third-degree

polynomial overtakes the second-degree polynomial, the performance gain is small. Therefore, the second-degree polynomial may be preferred for robustness with a smaller training set and simpler computation, with little loss in performance.

Figure 7 shows the misalignment vectors between peak-pairs in the GCx2GC chromatograms before and after alignment. The displacements before alignment increase both from bottom to top and from left to right. The affine transformation improves alignment for many peaks, but has errors visible in the upper left and lower right. Both the polynomial transformations improve alignment across the retention-times space.

Figure 8 shows the transformation functions applied to a uniform rectangular grid. With the affine transformation, the parallel lines for constant ^{2}D retention times remain parallel after the transformation, so the non-linear differences cannot be corrected. The polynomial transformations can track the nonlinear systemic differences and so outperform affine transformation.

Conclusions and Future Work. This research indicates that global, low-order polynomial transformations are effective for aligning chromatograms from GCx2GC with duplicate secondary columns and that they improve

on the performance of affine transformation. Second-degree polynomials performed nearly as well as third-degree polynomials and may be preferred for their simplicity, requirement of fewer landmark peak-pairs, and greater robustness for small sets of landmark peak-pairs. In the experiments here, although as few as 6 landmark peak-pairs are mathematically sufficient for determining the optimal second-degree polynomial, more than four times as many may be required for near peak-performance for points not in the training set. We expect that these conclusions also would hold for GCxGC with dual parallel detectors (e.g., GCxGC-FID/MS or other detector combinations) for which the 2D chromatograms may have differing retention-times patterns (e.g., due to differences in splitter performance, connecting capillaries, operative pressures, and/or detetectors). However, for GCx2GC with different stationary phases in the secondary columns, simple retention-time transformation models could be ill-suited (be they local or global). This research also makes contributions in methodologies for evaluating alignment performance: demonstrating the use of consecutive replicate runs to establish alignment benchmarks related to inherent noise and using cross-validation with variable-sized training sets to assess performance as a function of the number of points used for alignment.

Although it is not the subject of this work, alignment of GCxGC chromatograms from different runs also is an important problem. For example, GCxGC retention-times patterns change as columns age and differ from one system to another. Global low-order polynomial transformations can be applied to the problem of aligning different GCxGC chromatograms, (*17*) but their performance for different situations has not been investigated deeply. We have begun experiments that use the assessment methods described here to evaluate the performance of global, low-order polynomials for aligning GCxGC chromatograms in varied situations, with comparisons to local alignment methods.

The next version of GC Image Software will have facilities (a) to compute the optimal parameters for a second-degree polynomial model from matched points determined by template matching, (b) to update a template based on a second-degree polynomial function computed after template matching, and (c) to transform a chromatogram according to a set of matched points (e.g., those determined by template matching or any other method) using a second-degree polynomial function and a selected resampling method.

■ ASSOCIATED CONTENT

Supporting Information

Results for additional examples and additional statistical results are included in the Supporting Information. This material is available free of charge via the Internet at http://pubs.acs.org.

■ AUTHOR INFORMATION

Corresponding Author

* Email: reich@unl.edu.

Author Contributions

Samples were collected at La Sapienza University, Rome, Italy. GCx2GC analyses were performed at the Università degli Studi di Torino. Data analysis was performed at the University of Nebraska – Lincoln in collaboration with GC Image, LLC.

■ REFERENCES

(1) Seeley, J. V.; Kramp, F. J.; Sharpe, K. S. *J. Sep. Sci.* **2001**, *24*, 444-450.

(2) Seeley, J. V.; Kramp, F. J.; Sharpe, K. S.; Seeley, S. K. *J. Sep. Sci.* **2002**, *25*, 53-59.

(3) Nicolotti, L.; Cordero, C.; Bressanello, D.; Cagliero, C.; Liberto, E.; Magagna, F.; Rubiolo, P.; Sgorbini, B.; Bicchi, C. *J. Chromatogr. A* **2014**, *1360*, 264-275.

(4) Bressanello, D.; Liberto, E.; Collino, M.; Reichenbach, S. E.; Benetti, E.; Chiazza, F.; Bicchi, C.; Cordero, C. *J. Chromatogr. A* **2014**, *1361*, 265-276.

(5) Peroni, D.; Sampat, A. A. S.; van Egmond, W.; de Koning, S.; Cochran, J.; Lautamo, R.; Janssen, H.-G. *J. Chromatogr. A* **2013**, *1317*, 3-11.

(6) Peroni, D.; Janssen, H.-G. *J. Chromatogr. A* **2014**, *1332*, 57-63.

(7) Fraga, C. G.; Prazen, B. J.; Synovec, R. E. *Anal. Chem.* **2001**, *73*, 5833-5840.

(8) Sakoe, H.; Chiba, S. *IEEE Trans. Acoust., Speech, Signal Process.* **1978**, *26*, 43-49.

(9) Nielsen, N.-P.; Carstensen, J. M.; Smedsgaard, J. *J. Chromatogr. A* **1998**, *805*, 17-35.

(10) Vial, J.; Noçairi, H.; Sassiat, P.; Mallipatu, S.; Cognon, G.; Thiébaut, D.; Teillet, B.; Rutledge, D. N. *J. Chromatogr. A* **2009**, *1216*, 2866–2872.

(11) Zhang, D.; Huang, X.; Regnier, F. E.; Zhang, M. *Anal. Chem.* **2008**, *80*, 2664-2671.

(12) Wang, B.; Fang, A.; Helm, J.; Bogdanov, B.; Pugh, S.; Libardoni, M.; Zhang, X. *Anal. Chem.* **2010**, *82*, 5069-5081.

(13) Gros, J.; Nabi, D.; Dimitriou-Christidis, P.; Rutler, R.; Arey, J. S. *Anal. Chem.* **2012**, *84*, 9033-9040.

(14) Sibson, R. In *Interpreting Multivariate Data;* Barnett, V., Ed.; John Wiley & Sons: New York, 1981; pp 21–36.

(15) Furbo, S.; Hansen, A. B.; Skov, T.; Christensen, J. H. *Anal. Chem.* **2014**, *86*, 7160−7170.

(16) Ni, M.; Reichenbach, S. E.; Visvanathan, A.; TerMaat, J.; Ledford, E. B. *J. Chromatogr. A* **2005**, *1086*, 165–170.

(17) van Mispelaar, V. *Chromametrics;* Universal Press: Veenendaal NL, 2005.

(18) Zhang, Q.; Wang, G.; Du, Y.; Zhu, L.; Jiye, A. *J. Chromatogr. B* **2007**, *854*, 20-25.

(19) Reichenbach, S. E. In *Comprehensive Two Dimensional Gas Chromatography;* Ramos, L., Ed.; Elsevier, 2009; pp 77-106.

(20) GC Image, LLC. *GC Image GCxGC Software Users' Guide;* GC Image, LLC: Lincoln NE, 2015.

(21) Wolfram Research, Inc. Least Squares Fitting--Polynomial. http://mathworld.wolfram.com/LeastSquaresFittingPolynomial.html (accessed Aug 25, 2015).

Supporting Information for "Alignment for Comprehensive Two-Dimensional Gas Chromatography with Dual Secondary Columns and Detectors (GCx2GC)" [Submitted to *Analytical Chemistry*.]

Stephen E. Reichenbach,[*] Davis W. Rempe,[*] Qingping Tao,[†] Davide Bressanello,[‡] Erica Liberto,[‡] Carlo Bicchi,[‡] Stefano Balducci,[§] Chiara Cordero[‡]

*University of Nebraska – Lincoln, Lincoln NE 68588-0115, USA

†GC Image, LLC, Lincoln NE 68505-7403, USA

‡Università degli Studi di Torino, I-10125 Torino, Italy

§La Sapienza University, Rome, Italy

ABSTRACT: This document provides supporting information for the paper "Alignment for Comprehensive Two-Dimensional Gas Chromatography with Dual Secondary Columns and Detectors (GCx2GC)", for the journal *Analytical Chemistry*. Due to space constraints and for brevity of presentation, the body of that paper presents results for only a few examples. This supplement provides additional results. This supplement also presents results for the maximum alignment error, which supplements the results for the average alignment error presented in the body of the paper. For a description of the samples, instrumentation, system settings, data preprocessing, alignment algorithms, and evaluation methodology, as well as references, refer to the body of the paper.

Review of Local Alignment Methods for GCxGC. Many local alignment methods have been proposed for GCxGC chromatographic data. One of the earliest methods used simple retention-time shifting to realize minimum pseudorank, with interpolation of the data for subpixel shifts (7). Dynamic Time Warping (DTW) (8) and Correlation Optimized Warping (COW) (9) were originally applied to one-dimensional signals then adapted for GCxGC (10,11). DTW uses dynamic programming to define a non-linear warping path to align two signals. For GCxGC, Vial et al. (10) applied DTW to the more variable second-column chromatograms. In developing COW, Nielsen (9) noted that the DTW distance measure relies on similar peak heights in the two chromatograms to give a reliable alignment (or on extensive pretreatment). COW segments one of the signals and uses correlation to assess piecewise linear warping of each segment to align with the other signal. Dynamic programming is used to solve the combinatorial optimization for all segments to have consistent start and end points without overlaps or gaps. Zhang et al. (11) applied COW separably in two dimensions, effecting piecewise bilinear interpolation. Both of these local methods require time-consuming computations. Wang et al. (12) developed a local alignment algorithm based on landmark peaks using distance and spectrum correlation optimization (DISCO). Although DISCO was developed for peak matching, it defines a retention-times mapping function in which the retention-times plane is segmented using the positions of landmark peaks, then piecewise linear interpolation is used to interpolate the retention-times of non-landmark peaks. Gros et al. (13) developed a landmark-based local alignment algorithm using Sibson natural-neighbor interpolation (14), based on a Voronoi diagram defined by landmark peaks. Recently, Furbo et al. (15) developed a local alignment method in which the correlation-optimized shift for each second-dimension chromatogram is computed and then those shifts are fit by a polynomial function. These local methods have varying levels of representational power, but all are more computationally expensive than simple global methods and cannot simply capture global structure.

Additional Results for Calibration Chromatograms. Figure S1 shows the results for alignment of an additional pair of consecutive replicate calibration runs (with concentration 100 mg/L). The alignment of chromatograms from the same detector in consecutive replicate runs provide benchmarks for subsequent alignment of the chromatograms from the flame ionization detector (FID) and mass spectrometer (MS) from a single GCx2GC-FID/MS run. For consecutive replicate calibration runs 2 and 3, the ^{1}D misalignment is about 0.041 min (or $0.7 \times ^1\sigma$); and, the ^{2}D misalignment is about 0.043 sec (or $0.5 \times ^2\sigma$) for the MS (which has a lower sampling frequency than the FID). These benchmarks are in line with those in the paper (although slightly higher for ^{1}D).

Figure S2 illustrates the performance for aligning FID and MS GCx2GC chromatograms from the same calibration run. As expected, for ^{1}D, none of the models yields any improvement in the testing set. As for the example in the paper, the ^{1}D misalignment is approximately equal to the stochastic modulation sampling noise level (0.024 min). For ^{2}D, all of the transformation models significantly improved alignment from about 0.14 sec (or $1.6 \times ^2\sigma$) before transformation to about 0.05 sec (or $0.6 \times ^2\sigma$) or less, with the second-degree polynomial approaching the benchmark of 0.043 sec. These results are consistent with those presented in the paper.

Tables S1 and S2 document the retention times and ^{1}D linear retention indices (LRIs) of calibration compounds in run #1 before and after alignment for all methods.

Additional Results for Urine Sample Chromatograms. Figure S3 shows the alignment results for another pair of consecutive replicate runs of one of the urine samples, which are used to establish benchmarks. For ^{1}D, the benchmark is about 0.026 min (or about $0.4 \times ^1\sigma$); and, for ^{2}D, the benchmark is about 0.038 sec (or about $0.4 \times ^2\sigma$) for the MS (which has a lower sampling frequency than the

FID). These results are in line with those in the paper (although slightly higher for ^{2}D).

Figure S4 shows the alignment performance for two GCx2GC runs of a urine sample. For ^{1}D, the misalignment of the FID and MS chromatograms is at the benchmark (about 0.03 min or $0.5 \times {}^1\sigma$) without transformation and, as expected, none of the models reduces misalignment. For ^{2}D, the misalignment before transformation is large, about 0.25 sec or $2.9 \times {}^2\sigma$, several times the benchmark. All of the transformation models significantly improve alignment. Affine transformation reduces misalignment by about two-thirds, to 0.09 sec (or $1.0 \times {}^2\sigma$), but does not achieve the benchmark. Both polynomial transformations reduce misalignment to about 0.035 sec (or $0.4 \times {}^2\sigma$), which is the benchmark for consecutive replicate sample runs. These results are consistent with those presented in the paper.

Maximum Alignment Error. Results for the root-mean-square error (RMSE) indicate average performance. The worst-case error also is of interest. Figures S5–S7 present the maximum absolute alignment error for any peak pair in any of the cross-validation runs for GCx2GC alignment, with Figure S5 for the calibration runs, Figure S6 for sample 41 runs, Figure S7 for sample 50 runs.

In all of these graphs, the size of the training set increases from left to right and the size of the testing set decreases from left to right, so there generally is an increase in the maximum error from left to right in the training set and a decrease in the maximum error in the testing set. Those trends are not of interest. Instead, the graphs should be viewed with an eye to the relative performance indicated by the four lines.

For ^{1}D, in all of the examples, if the training set is large enough, then the maximum absolute error for the testing set is about the same for all functions. For 2D, if the training set is large enough, then the maximum absolute error for the testing set is reduced by the affine transformation but is not as small as for the second-degree and third-degree polynomials, which perform similarly. As expected, the affine transformation requires the smallest training set and the third-degree polynomial requires the largest training set. These worst-case results are consistent with the results for mean performance. Also, the standard deviation of the maximum absolute error (computed over the iterations of leave-one-out cross-validation) was reduced by the affine transform but is not as small as for the second-degree and third-degree polynomials.
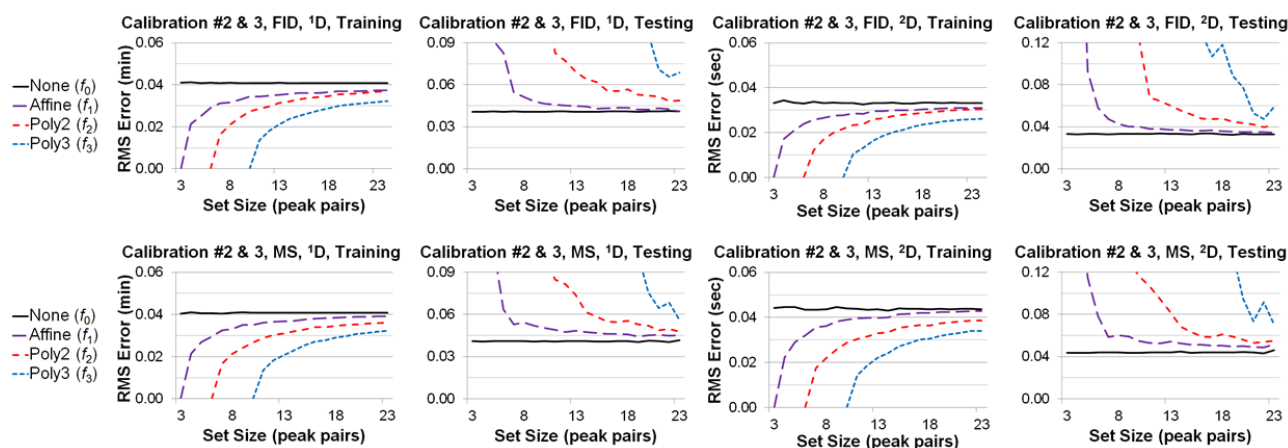
Figure S1: Cross-validation RMSE results as a function of the training set size for alignment of consecutive, replicate calibration chromatograms from the same detector. Columns from left to right are for ^1D with the training set, for ^1D with the testing set, for ^2D with the training set, and for ^2D with the testing set. The top row is for the FID chromatograms of calibration runs #2 and #3 and the bottom row is for the MS chromatograms of calibration runs #2 and #3.
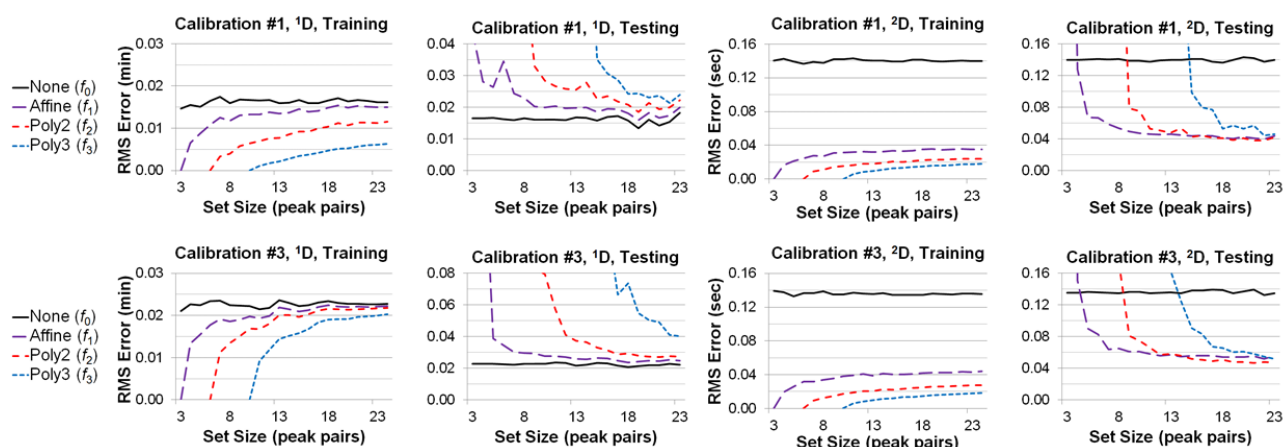

Figure S2: Cross-validation RMSE results as a function of the training set size for alignment of GCx2GC calibration chromatograms (from different detectors). Columns from left to right are for ^1D with the training set, for ^1D with the testing set, for ^2D with the training set, and for ^2D with the testing set. The top row is for the FID and MS chromatograms of calibration run #1 and the bottom row is for the FID and MS chromatograms of calibration run #3.
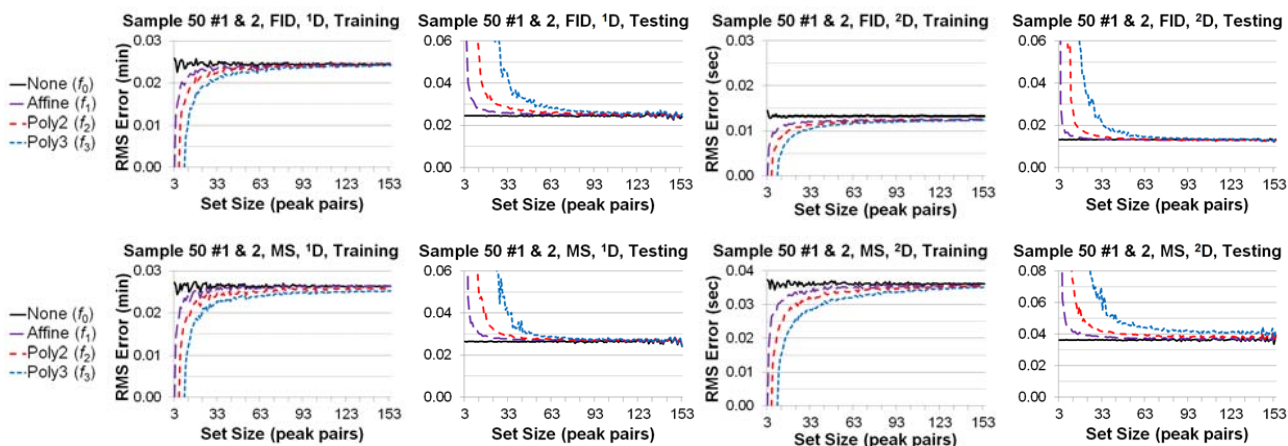
Figure S3: Cross-validation RMSE results as a function of the training set size for alignment of consecutive, replicate urine sample chromatograms from the same detector. Columns from left to right are for ^1D with the training set, for ^1D with the testing set, for ^2D with the training set, and for ^2D with the testing set. The top row is for the FID chromatograms of sample 50, runs #1 and #2, and the bottom row is for the MS chromatograms of sample 50, runs #1 and #2.
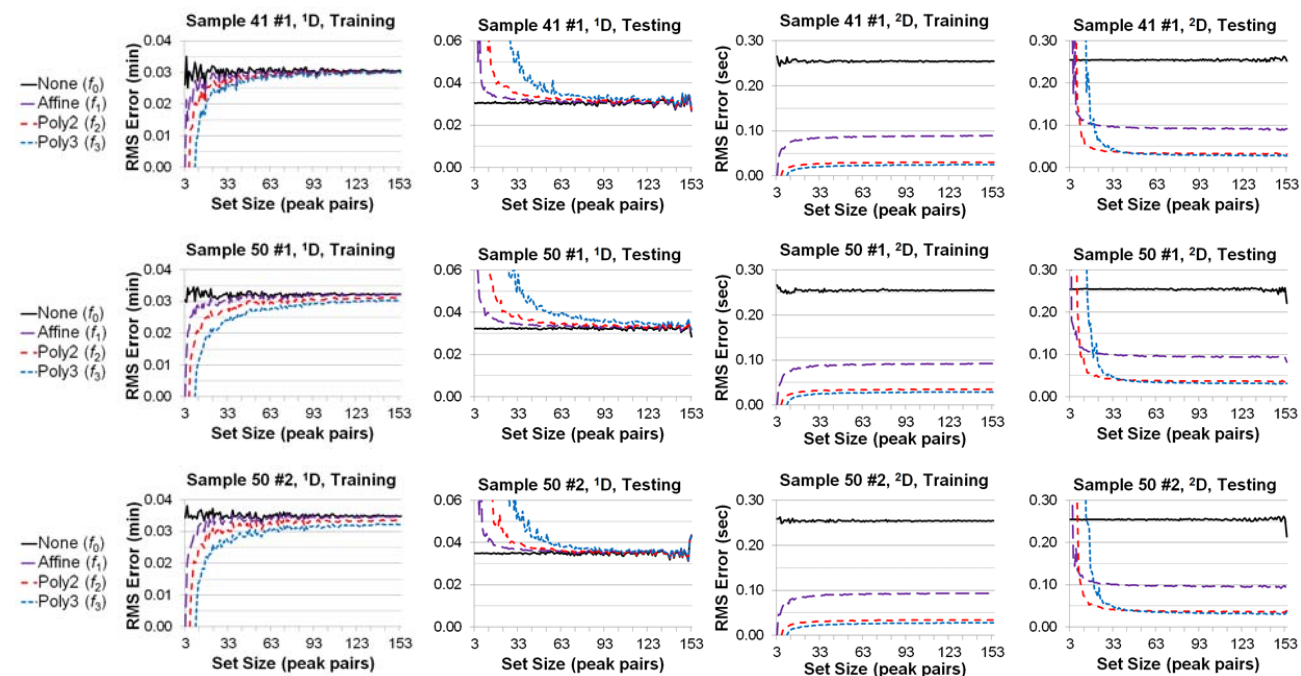

Figure S4: Cross-validation RMSE results as a function of the training set size for alignment of GCx2GC urine sample chromatograms (from different detectors). Columns from left to right are for ^1D with the training set, for ^1D with the testing set, for ^2D with the training set, and for ^2D with the testing set. Rows from top to bottom are for the FID and MS chromatograms of sample 41, run #1; for the FID and MS chromatograms of sample 50, run #1; and for the FID and MS chromatograms of sample 50, run #2.

A. Calibration #1.

B. Calibration #2.

C. Calibration #3.

Figure S5: Maximum absolute error as a function of the training set size for alignment of GCx2GC calibration chromatograms (from different detectors). Columns from left to right are for ^1D with the training set, for ^1D with the testing set, for ^2D with the training set, and for ^2D with the testing set. Sets of rows with maximum absolute error on the top row of each set and the standard deviation of maximum absolute error on the bottom row of each set are for: A. Calibration #1, B. Calibration #2, and C. Calibration #3.

A. Sample 41, Run #1.

B. Sample 41, Run #2.
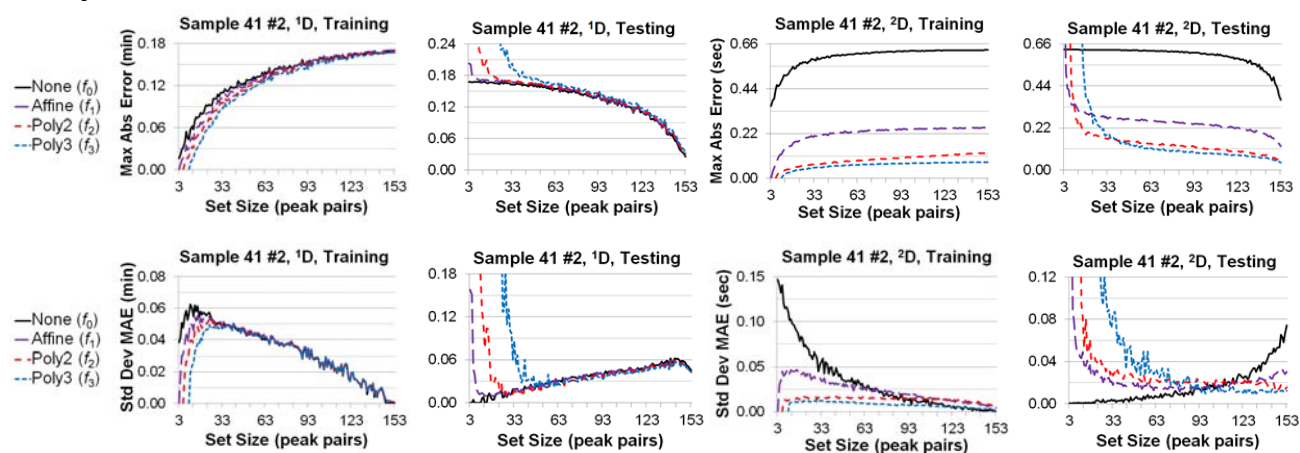
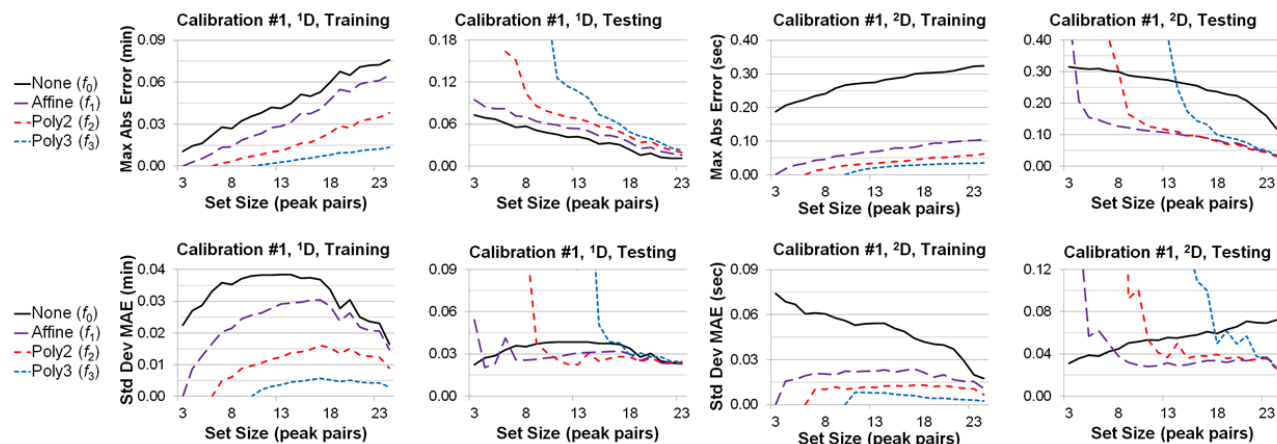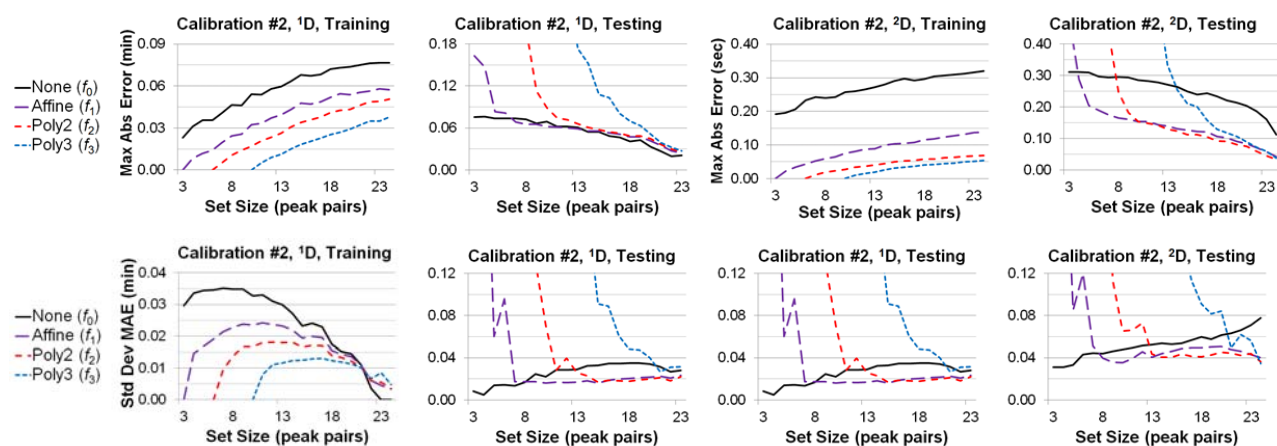*Figure S6: Maximum absolute error as a function of the training set size for alignment of GCx2GC urine sample #41 chromatograms (from different detectors). Columns from left to right are for ^1D with the training set, for ^1D with the testing set, for ^2D with the training set, and for ^2D with the testing set. Sets of rows with maximum absolute error on the top row of each set and the standard deviation of maximum absolute error on the bottom row of each set are for: A. Sample 41, Run #1, and B. Sample 41, Run #2.*

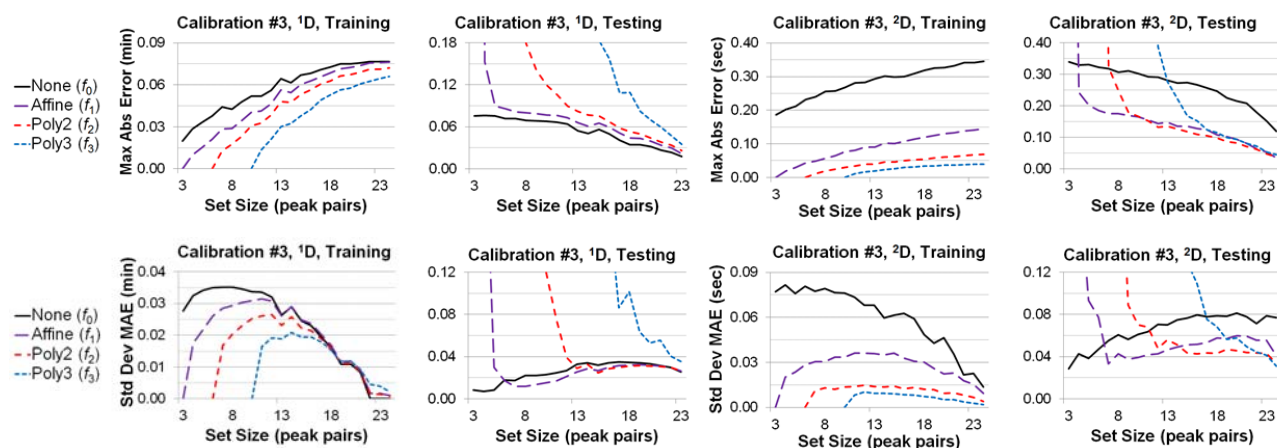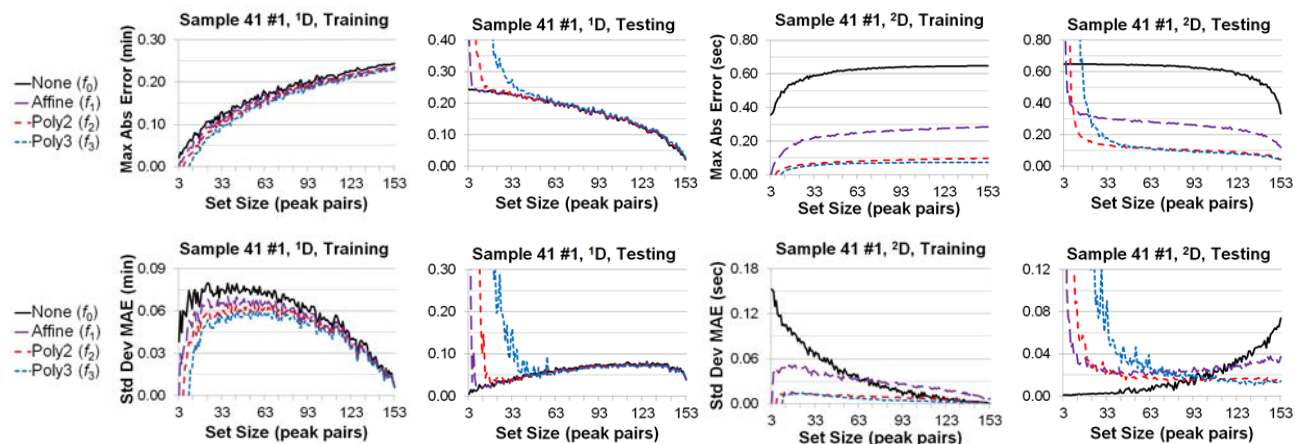C. Sample 50, Run #1.
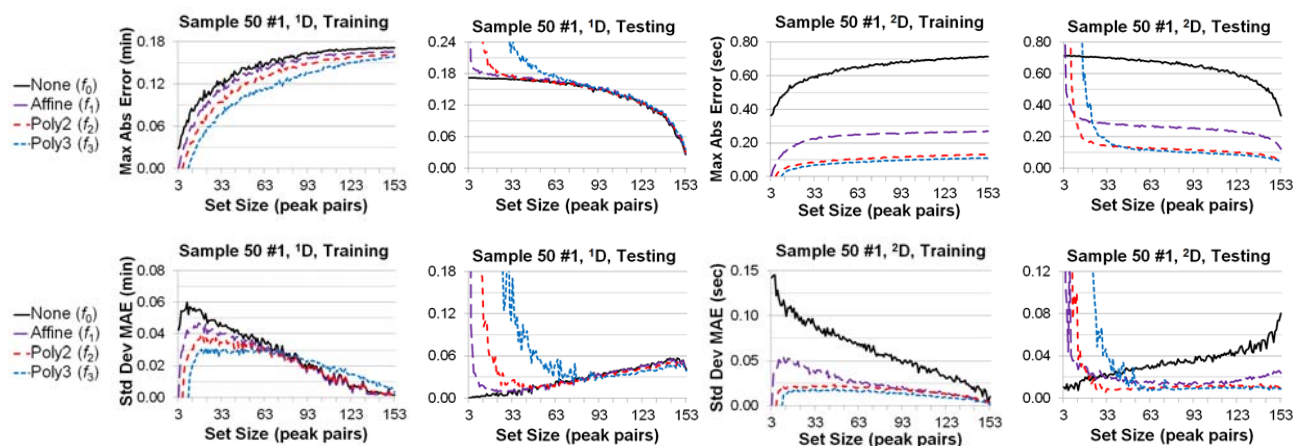
D. Sample 50, Run #2.
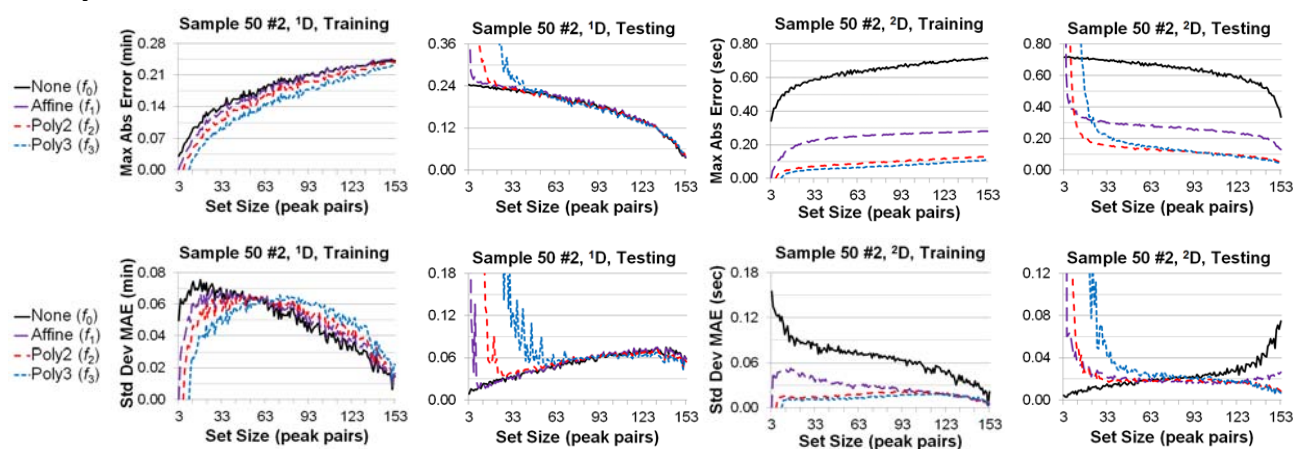
Figure S7: Maximum absolute error as a function of the training set size for alignment of GCx2GC urine sample #50 chromatograms (from different detectors). Columns from left to right are for ^{1}D with the training set, for ^{1}D with the testing set, for ^{2}D with the training set, and for ^{2}D with the testing set. Sets of rows with maximum absolute error on the top row of each set and the standard deviation of maximum absolute error on the bottom row of each set are for: A. Sample 50, Run #1, and B. Sample 50, Run #2.

Table S1 Transformations of the 25 target peaks in calibration #1 from the GCx2GC-MS chromatogram to align with corresponding peaks from the GCx2GC-FID chromatogram.

Compound Name	FID (f_0)			MS→FID Affine (f_1)			MS→FID Poly2 (f_2)			MS→FID Poly3 (f_3)		
	1D Rt (min)	2D Rt (sec)	1D LRI	1D Rt (min)	2D Rt (sec)	1D LRI	1D Rt (min)	2D Rt (sec)	1D LRI	1D Rt (min)	2D Rt (sec)	1D LRI
Pyruvic acid	8.92	3.50	1070	8.92	3.53	1070	8.91	3.54	1070	8.92	3.52	1070
Lactic acid	9.25	3.35	1081	9.25	3.35	1081	9.25	3.33	1081	9.25	3.33	1081
Alanine	10.58	3.32	1122	10.59	3.33	1122	10.58	3.31	1122	10.58	3.31	1122
Malonic acid	14.00	4.40	1224	14.00	4.33	1224	13.99	4.41	1223	14.01	4.41	1224
Valine	14.33	3.40	1233	14.34	3.38	1233	14.33	3.38	1233	14.33	3.38	1233
Leucine	16.33	3.40	1290	16.33	3.41	1290	16.33	3.42	1290	16.33	3.43	1290
Glycerol	16.67	2.89	1300	16.67	2.93	1300	16.68	2.89	1300	16.67	2.91	1300
Proline	16.92	3.49	1307	16.92	3.47	1307	16.92	3.49	1307	16.92	3.49	1307
Glycine	17.33	3.24	1320	17.33	3.26	1320	17.34	3.26	1320	17.33	3.26	1320
Succinic acid	17.67	4.25	1330	17.67	4.17	1330	17.67	4.22	1330	17.66	4.23	1330
Threonine	20.42	3.18	1413	20.42	3.18	1413	20.42	3.17	1413	20.41	3.18	1413
Malic acid	23.75	3.58	1515	23.75	3.54	1515	23.75	3.54	1515	23.76	3.54	1515
Creatinine	25.33	3.54	1564	25.33	3.55	1564	25.33	3.54	1564	25.34	3.54	1564
2-Ketoglutaric acid	26.33	3.73	1595	26.33	3.81	1595	26.34	3.79	1595	26.32	3.79	1594
Phenylalanine	27.50	3.64	1629	27.50	3.62	1629	27.50	3.60	1629	27.50	3.60	1629
Xylitol	30.75	2.31	1725	30.74	2.31	1725	30.75	2.29	1725	30.76	2.28	1725
Ribitol	31.25	2.27	1740	31.24	2.27	1740	31.25	2.26	1740	31.26	2.24	1740
ISTD (F-Phe)	32.50	3.44	1777	32.49	3.54	1777	32.50	3.49	1777	32.50	3.49	1777
Hippuric Acid	33.67	0.81	1813	*	*	*	*	*	*	*	*	*
Tyrosine I[a]	35.08	3.49	1859	35.08	3.50	1859	35.08	3.44	1859	35.08	3.44	1859
Fructose	35.83	1.90	1884	35.82	1.90	1883	35.83	1.91	1883	35.84	1.90	1884
Glucose	36.58	1.92	1909	36.57	1.92	1908	36.57	1.93	1908	36.58	1.93	1909
Mannitol	37.00	1.91	1924	36.99	1.91	1924	36.99	1.93	1924	36.99	1.93	1924
Tyrosine II[b]	37.00	2.55	1924	36.99	2.59	1924	36.97	2.59	1923	36.99	2.58	1924
Galactose	37.50	1.81	1942	37.49	1.80	1942	37.49	1.83	1942	37.49	1.83	1942
Myo Inositol	41.83	1.91	2110	41.90	1.80	2113	41.87	1.86	2112	41.84	1.89	2111

* Wraparound peak not included in transformation.
[a] Derivative I: trimethylsilyl ester of O-trimethylsilyl-tyrosine
[b] Derivative II: trimethylsilyl ester of N,O-bis(trimethylsilyl)-tyrosine

Table S2 Transformations of the 25target peaks in calibration #1 from the GCx2GC-FID chromatogram to align with corresponding peaks from the GCx2GC-MS chromatogram.

Compound Name	MS Full-Scan (f_0)			FID→MS Affine (f_1)			FID→MS Poly2 (f_2)			FID→MS Poly3 (f_3)		
	¹D Rt (min)	²D Rt (sec)	¹D LRI	¹D Rt (min)	²D Rt (sec)	¹D LRI	¹D Rt (min)	²D Rt (sec)	¹D LRI	¹D Rt (min)	²D Rt (sec)	¹D LRI
Pyruvic acid	8.92	3.70	1070	8.92	3.66	1070	8.93	3.65	1071	8.92	3.68	1070
Lactic acid	9.25	3.48	1081	9.25	3.48	1081	9.26	3.50	1081	9.26	3.51	1081
Alanine	10.59	3.48	1123	10.59	3.47	1122	10.59	3.49	1123	10.59	3.49	1123
Malonic acid	14.00	4.80	1224	14.00	4.89	1224	14.01	4.78	1224	14.00	4.80	1224
Valine	14.34	3.61	1233	14.34	3.64	1233	14.34	3.64	1233	14.34	3.63	1233
Leucine	16.34	3.70	1290	16.34	3.68	1290	16.34	3.68	1291	16.34	3.67	1291
Glycerol	16.67	3.10	1300	16.67	3.04	1300	16.65	3.11	1299	16.67	3.09	1300
Proline	16.92	3.78	1308	16.92	3.80	1307	16.92	3.79	1308	16.92	3.79	1307
Glycine	17.34	3.53	1320	17.34	3.50	1320	17.33	3.51	1320	17.34	3.49	1320
Succinic acid	17.67	4.67	1330	17.67	4.77	1330	17.67	4.71	1330	17.68	4.68	1330
Threonine	20.42	3.48	1413	20.42	3.48	1413	20.42	3.50	1413	20.42	3.48	1413
Malic acid	23.75	3.99	1515	23.76	4.05	1515	23.75	4.05	1515	23.75	4.06	1515
Creatinine	25.34	4.04	1564	25.34	4.03	1564	25.34	4.03	1564	25.33	4.05	1564
2-Ketoglutaric acid	26.34	4.38	1595	26.34	4.29	1595	26.33	4.30	1595	26.34	4.29	1595
Phenylalanine	27.50	4.16	1629	27.51	4.20	1629	27.50	4.22	1629	27.50	4.22	1629
Xylitol	30.75	2.59	1725	30.76	2.59	1725	30.75	2.61	1725	30.75	2.61	1725
Ribitol	31.25	2.55	1740	31.26	2.54	1740	31.25	2.57	1740	31.25	2.57	1740
ISTD (F-Phe)	32.50	4.16	1778	32.51	4.04	1778	32.51	4.08	1778	32.50	4.10	1777
Hippuric Acid	33.67	0.81	1813	*	*	*	*	*	*	*	*	*
Tyrosine I[a]	35.09	4.16	1859	35.09	4.15	1860	35.09	4.22	1860	35.09	4.20	1860
Fructose	35.84	2.17	1884	35.85	2.17	1884	35.84	2.16	1884	35.83	2.18	1884
Glucose	36.59	2.21	1909	36.60	2.21	1910	36.60	2.19	1909	36.59	2.20	1909
Mannitol	37.00	2.21	1924	37.02	2.20	1925	37.02	2.18	1925	37.02	2.18	1925
Tyrosine II[b]	37.00	3.06	1924	37.02	3.01	1925	37.03	3.01	1925	37.02	3.03	1925
Galactose	37.50	2.08	1942	37.52	2.09	1943	37.52	2.06	1943	37.51	2.07	1943
Myo Inositol	41.92	2.17	2114	41.85	2.30	2111	41.88	2.24	2112	41.91	2.19	2114

* Wraparound peak not included in transformation.
[a] Derivative I: trimethylsilyl ester of O-trimethylsilyl-tyrosine
[b] Derivative II: trimethylsilyl ester of N,O-bis(trimethylsilyl)-tyrosine